

Glacial Mediterranean sea surface temperatures based on planktonic foraminiferal assemblages

Angela Hayes^{a,b,*}, Michal Kucera^b, Nejb Kallel^c, Laura Sbaffi^d, Eelco J. Rohling^e

^aDepartment of Geography, Mary Immaculate College, University of Limerick, Limerick, Ireland

^bDepartment of Geology, Royal Holloway University of London, Egham, Surrey TW20 0EX, UK

^cLaboratoire E08/C10, Faculte des sciences de Sfax, Route de Soukra, B.P. 763, 3038 Sfax, Tunisia

^dGeoscience Australia, Petroleum & Marine division, GPO Box 378, Canberra ACT 2601, Australia

^eSouthampton Oceanography Centre, School of Ocean & Earth Science, Southampton SO14 3ZH, UK

Received 8 September 2003; accepted 10 February 2004

Abstract

We present a new reconstruction of Mediterranean sea surface temperatures (SST) during the last glacial maximum (LGM). A calibration data set based on census counts of 23 species of planktonic foraminifera in 129 North Atlantic and 145 Mediterranean core top samples was used to develop summer, winter and annual average SST reconstructions using artificial neural networks (ANNs) and the revised analogue method (RAM). Prediction errors determined by cross-validation of the calibration data set ranged between 0.5 and 1.1 °C, with both techniques being most successful in predicting winter SSTs. Glacial reconstructions are based on a new, expanded data set of 273 samples in 37 cores with consistent minimum level of age control.

The new LGM reconstructions suggest that the east–west temperature gradient during the glacial summer was 9 °C, whereas during the glacial winter, the gradient was 6 °C, both some 4 °C higher than that existing today. In contrast to earlier studies, our results tend to suggest much cooler SST estimates throughout the glacial Mediterranean, particularly in the eastern basin where previous SST reconstructions indicated a decrease of only 1 °C. Our new SST reconstructions will provide the modelling community with a detailed and updated portrayal of the Mediterranean Sea during the LGM, setting new targets on which glacial simulations can be tested.

© 2004 Elsevier Ltd. All rights reserved.

1. Introduction

The last glacial maximum (LGM) is a period in geological time that represents a climate dramatically different from that of today. Sea surface temperature (SST) reconstructions during this interval have become the main target of many palaeoceanographic studies since they provide valuable information required for modelling climate and ocean circulation. The use of planktonic foraminifera as a SST proxy was recognised much earlier. Murray (1897) identified that specific

faunal assemblages provided clues to the temperature of the water they lived in. Schott (1935) introduced quantitative counting of species within the assemblages. He recognised that species compositions vary downcore, concluding that surface water temperatures changed as the climate fluctuated between glacial and interglacial periods. Since then, planktonic foraminifera have become a widely used proxy for determining SST reconstructions on a global scale (CLIMAP, 1976; Sarthein et al., 2003).

Situated in a subtropical semi-arid climate, the Mediterranean Sea is a semi-enclosed basin with the Strait of Gibraltar providing the only connection to the open ocean. Due to its subtropical location, the Mediterranean Sea receives much solar radiation, which along with the prevailing eastward surface circulation

*Corresponding author. Department of Geography, Mary Immaculate College, University of Limerick, Limerick, Ireland. Tel.: +353-61-204577; fax: +353-61-313632.

E-mail address: angela.hayes@mic.ul.ie (A. Hayes).

causes a strong west–east temperature gradient (Fig. 1). An excess of evaporation over precipitation furthermore results in a strong salinity increase from west to east (Wüst, 1961). Net buoyancy loss maintains a two-layer flow regime through the Strait of Gibraltar, consisting of Atlantic surface water inflow and Mediterranean subsurface water outflow (Lacombe et al., 1981; Lacombe and Richez, 1982; Pistek et al., 1985). The well-constrained hydrological balance in the Mediterranean Sea makes the basin an ideal location for testing mesoscale climate and ocean circulation models under both modern and past climate forcing conditions (Bigg, 1994; Myers et al., 1998; Myers and Rohling, 2000).

Mediterranean planktonic foraminifera have been extensively studied since the recovery of the first piston cores during the Swedish Deep Sea Expedition of 1946–47. Many authors have since produced qualitative palaeoclimatic reconstructions based on the distribution of planktonic faunal assemblages throughout the Quaternary (e.g. Parker, 1958; Todd, 1958; Olausson,

1960, 1961; Herman, 1972; Cita et al., 1977; Vergnaud-Grazzini et al., 1977; Thunell, 1978; Rohling et al., 1993a, 1995; Hayes et al., 1999; Buccheri et al., 2002). Several methods have been developed to quantify the relationship between planktonic faunal assemblages and the physical characteristics of overlying water masses (Malmgren et al., 2001). Two of these methods have been used for SST reconstructions in the Mediterranean Sea. The first of these, known as the Imbrie–Kipp transfer function (IKTF), uses the Q-mode principal component analysis to reduce species abundances into statistically independent end-member assemblages that are then regressed onto the environmental parameters (Imbrie and Kipp, 1971). The second technique, known as the modern analogue technique (MAT) (Hutson, 1980) uses an alternative approach: rather than generating a unique calibration formula, this method searches a database of modern faunal assemblages, extracting those that best resemble the fossil assemblage. The environmental parameters associated with the modern assemblages are then used to reconstruct those for the fossil sample (Hutson, 1980). Both methods have been fundamental in efforts to estimate Quaternary sea surface temperatures in the Mediterranean Sea (e.g. Thiede, 1978; Thunell, 1979; Kallel et al., 1997b; Gonzalez-Donoso et al., 2000; Sbaffi et al., 2001; Perez-Folgado et al., 2003). However, most of these recent studies have been limited to single-core palaeoclimatic reconstructions rather than multi-core analysis on a basin-wide scale.

CLIMAP (1976) presented the first attempt to quantify glacial sea surface temperatures across the entire Mediterranean Sea. The LGM interval was defined at 18,000 yr BP based on the maximum extent of continental glaciers and a combination of biostratigraphic, geochemical and isotopic evidence. The calibration data set was composed of both Mediterranean (Parker, 1958; Todd, 1958) and Atlantic (CLIMAP, 1976) core top samples and included counts of 22 planktonic foraminiferal species. Using the IKTF, CLIMAP reconstructed glacial SSTs producing a standard error of estimate of $\pm 1.38^\circ\text{C}$. However, due to taxonomic discrepancies and uncertain LGM stratigraphy, the reliability and precision of the reconstructions has been disputed (Thunell, 1979). Thiede (1978) used a similar approach to produce glacial winter and summer sea surface temperature estimates based on 33 cores (Figs. 2A and B). However, his reconstructions were derived from transfer functions based entirely on a North Atlantic calibration data set (Molina-Cruz and Thiede, 1978), which only provides modern analogues for glacial faunal assemblages in the western Mediterranean Sea. Conversely, a calibration data set composed entirely of Mediterranean samples will only provide analogues for the eastern Mediterranean glacial assemblages and exclude the western basin. Thiede's (1978)

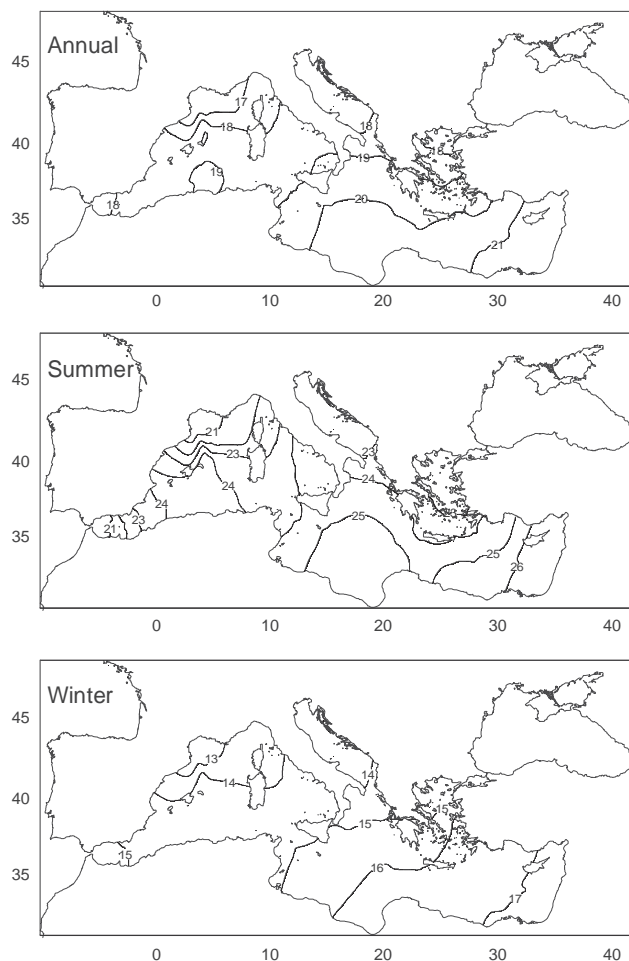


Fig. 1. Present day distribution of annual, summer and winter sea-surface temperatures at 10 m depth in the Mediterranean (data from the World Ocean Atlas 98, vol. 2).

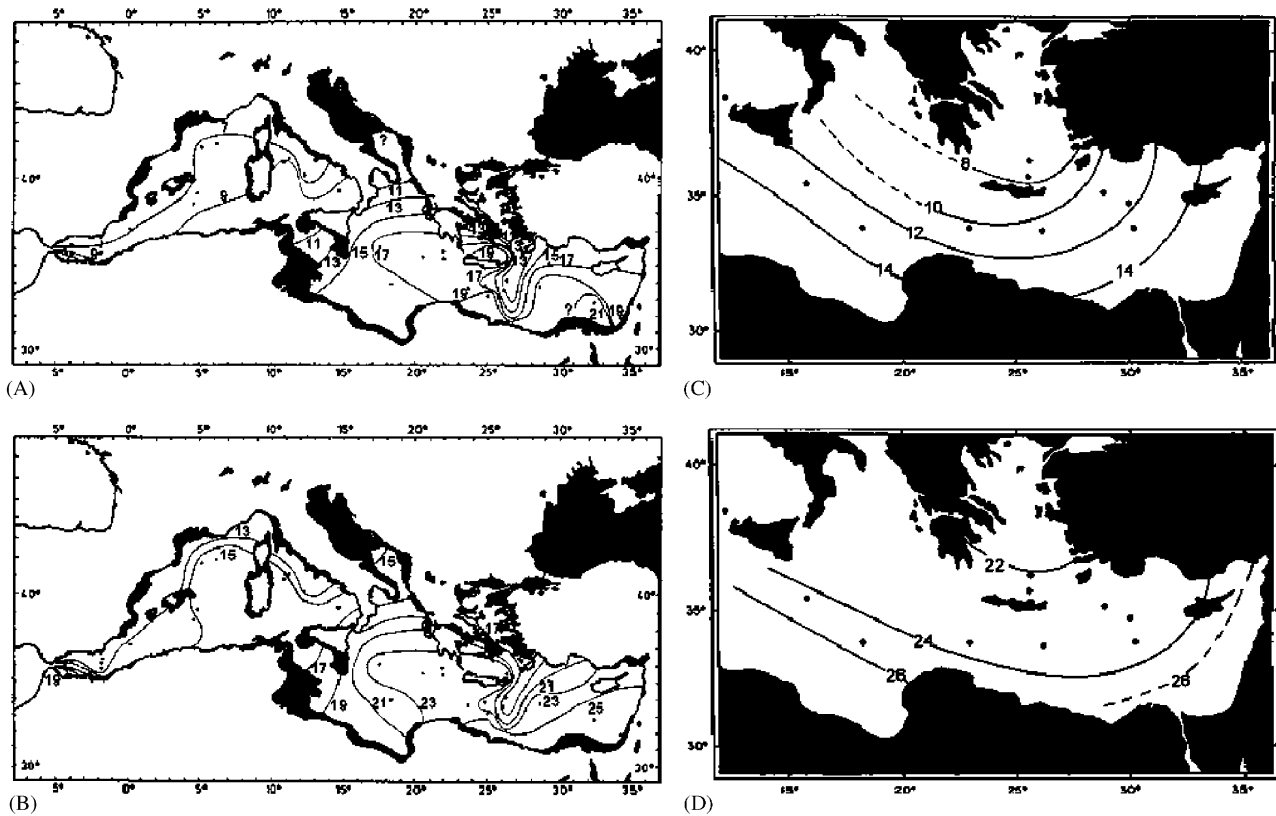


Fig. 2. Sea surface temperatures estimates for the glacial Mediterranean at 18,000 yr B.P. by Thiede (1978). (A) Glacial winter (February). (B) Glacial summer (August) and Thunell (1979) (C) Glacial winter. (D) Glacial summer. Black dots indicate core localities used for glacial reconstruction.

results displayed temperature values ranging from 7 °C in the north–west of the basin to >20 °C in the south–east during the glacial winter (Fig. 2A). During the summer, the reconstructed temperatures were significantly higher recording a range between 13 °C in the north–west to approximately 25 °C in the south–east (Fig. 2B). In a subsequent study, Thunell (1979) established a calibration data set composed of 66 Mediterranean and 8 North Atlantic trigger-weight cores. Applying the IKTF, faunal counts (21 species) from 10 piston cores enabled the reconstruction of eastern Mediterranean SSTs during the LGM (Figs. 2C and D). The standard error of estimates for summer and winter temperatures were 1.0 and 1.2 °C, respectively, and the LGM interval was defined on the basis of faunal stratigraphy, oxygen isotope stratigraphy and radiometric dates, providing a better age control than that used by Thiede (1978). Thunell's (1979) glacial summer temperatures were similar to those suggested by Thiede (1978), ranging between 22 and 26 °C (Fig. 3D). However, discrepancies between the two studies are more noticeable during the glacial winter with Thunell (1979) estimating temperatures between 8 and 14 °C (Fig. 3C), some 5 °C lower than those of Thiede (1978).

In recent years, the need for improvement in the precision and reliability of SST estimates has led to the development of new transfer function techniques. Specifically, improvements in the MAT include the modern analogue with a similarity index (SIMMAX) method (Pflaumann et al., 1996) and the revised analogue method (RAM) (Waelbroeck et al., 1998). A further approach relies on the concept of artificial neural networks (ANN), a computer-intensive method based on unsupervised learning of a relationship between two sets of variables (Malmgren and Nordlund, 1997; Malmgren et al., 2001).

The purpose of this paper is to provide an updated, detailed and comprehensive reconstruction of Mediterranean SSTs during the LGM. For the first time in a quarter of a century, we aim to provide SST reconstructions of consistent quality and reliability across the entire Mediterranean Sea. We use the ANN technique as a basis for our reconstructions, and the RAM for a comparison. The ANN has proved effective in providing reliable palaeoestimates compared to conventional computational techniques (Malmgren et al., 2001). Using a larger, more constrained calibration data set, a new, expanded fossil data set and a combination of two computational techniques (ANN and RAM), we

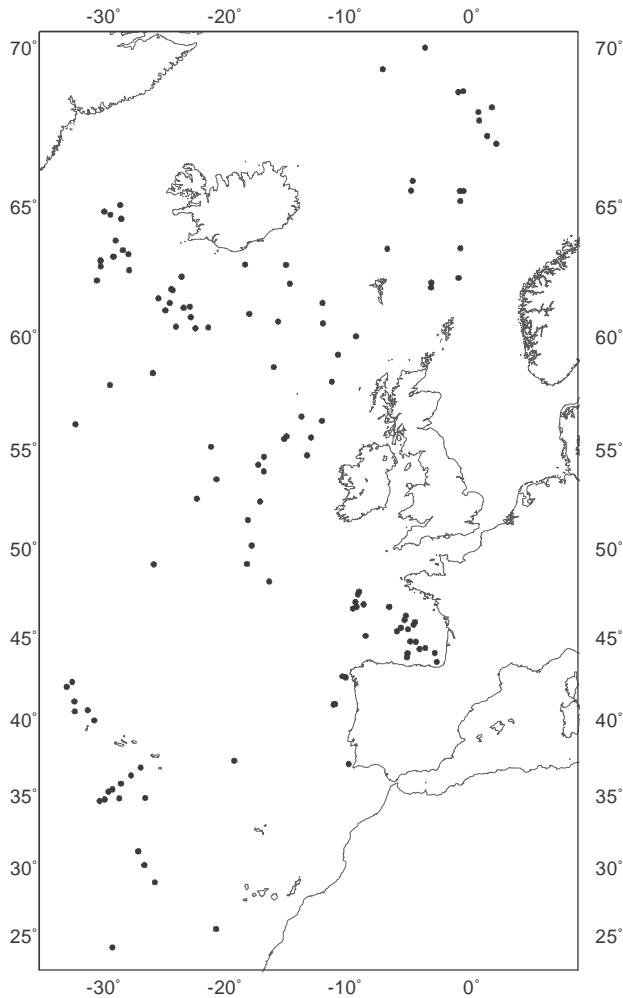


Fig. 3. Map illustrating the core localities in the North Atlantic portion of the calibration data set used in this study (taken from North Atlantic database presented in Kucera et al., 2004b).

believe that our reconstruction will provide an accurate portrayal of the glacial Mediterranean, providing more reliable surface forcing fields for numerical modelling studies.

2. Materials

2.1. Calibration data set

The calibration data set used in this study is based on census counts of planktonic foraminiferal species in 274 core tops from the North Atlantic Ocean (Fig. 3) and the Mediterranean Sea (Fig. 4). The Mediterranean data set contains 145 core tops, 32 of which are additional to those presented by Thunell (1978) and Kallel et al. (1997b) (Tables 1 and 2). The remaining 129 cores are taken from the North Atlantic database presented in Kucera et al. (2004b), which is an updated version of the

GLAMAP data set presented in Pflaumann et al. (2003). The North Atlantic core tops are included to provide analogues for glacial Mediterranean assemblages, which contain species that do not occur in the Mediterranean today. Intuitively, it would seem advantageous to include in the training database as many Atlantic samples as possible, covering the widest range of environments encountered in this part of the world today. There are, however, two main reasons to avoid such approach. Firstly, all the commonly used transfer function techniques derive an environmental calibration on the basis of finding the minimum total error of prediction. If one part of the ocean or one part of the range of an environmental variable is over represented, the techniques may produce calibrations preferentially minimising the error in the over represented set of samples, whilst allowing larger errors to occur elsewhere. Secondly, morphologically defined species of planktonic foraminifera (morphospecies) are known to consist of complexes of genetically and ecologically distinct types; the lumping of these types into morphospecies is a likely source of a significant portion of the error rate of foraminifer-based transfer functions (Kucera and Darling, 2002). Many of the cryptic genetic types have geographically distinct distributions (Kucera and Darling, 2002). Therefore, limiting the spatial extent of the calibration data set should decrease the degree of lumping of these ecologically distinct units and improve the error rate of a transfer function.

With these two assumptions in mind, all of the Atlantic core tops that were included into the calibration database were selected within the latitudinal range of approximately 25–70°N and longitudinal range of 5°E–30°W. This encompasses an area small enough within the North Atlantic to reduce the effect of lumping of cryptic genetic types but large enough to include assemblages from subpolar–polar water masses which may have existed in the glacial Mediterranean (Rohling et al., 1998). Samples from upwelling areas were excluded since they produce specific opportunistic faunal assemblages determined by uncharacteristic physical parameters (e.g. Ufkes et al., 1998). Similarly, core tops recording high percentages (>70%) of *Neogloboquadrina pachyderma* (left-coiling) were also omitted since such assemblages have never been observed in the Mediterranean Sea.

All samples within the calibration data set were picked from the > 150 µm size fraction. Total planktonic foraminiferal assemblages were quantified in relative abundances from splits containing approximately 300 specimens. A total of 23 species were counted in each sample (Table 5). Species selection was determined by the history of taxonomic practice of individual authors. For example, *Globigerinoides ruber* is commonly categorised into pink and white varieties. However, Thunell (1978) recorded both varieties collectively, therefore to

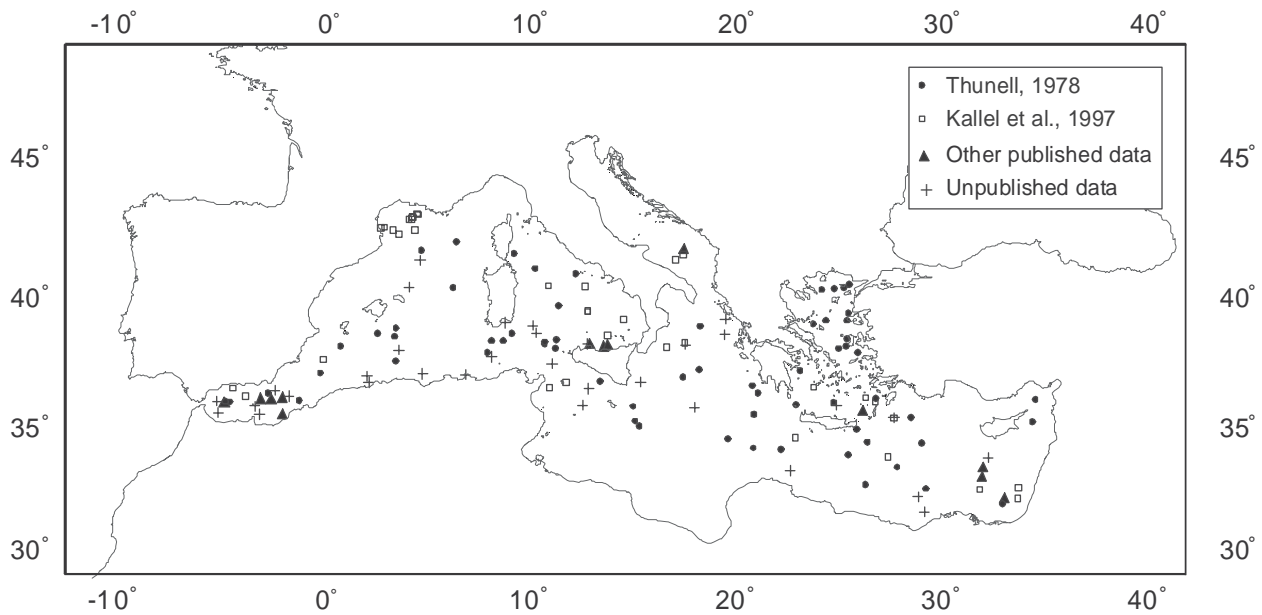


Fig. 4. Map illustrating the core localities in the Mediterranean portion of the calibration data set used in this study. Refer to Tables 1 and 2 for source details.

Table 1

Summary of core top samples used in the Mediterranean calibration data set taken from published sources in addition to samples published by Thunell (1978) and Kallel (1997b)

Core	Latitude	Longitude	Water depth (m)	Age quality	Data source
MD84-627	32.14	33.45	1185	3	Paterne et al. (1986)
MD84-639	33.40	32.42	870	3	Paterne et al. (1986)
MD84-641	33.02	32.38	1375	3	Paterne et al. (1986)
KS8232	36.11	-2.12	1920	3	Pujol and Vergnaud-Grazzini (1989)
KC8241	35.98	-4.40	1282	2	Pujol and Vergnaud-Grazzini (1989)
IN68-9	41.79	17.91	1234	2	Jorissen et al. (1993)
KS310	35.55	-1.57	1900	4	Rohling et al. (1995)
LC21	35.66	26.58	1522	2	Hayes et al. (1999)
BS79-22	38.23	14.23	1449	4	Sbaffi et al. (2001)
BS79-33	38.16	14.02	1282	4	Sbaffi et al. (2001)
BS79-38	38.25	13.35	1489	4	Sbaffi et al. (2001)
MD95-2043	36.14	-2.62	1841	1	Perez-Folgado et al. (2003)
ODP 977	36.19	-1.57	1984	1	Perez-Folgado et al. (2003)

achieve consistency within the data set we have grouped the pink and white varieties of *G. ruber* into one taxonomic category. For the same reasons, we have also grouped *Globigerinella siphonifera* with *Globigerinella calida*, *Globorotalia menardii* with *Globorotalia tumida* and “P/D intergrades” with *Neogloboquadrina pachyderma* (dextral).

For the purpose of calibration, winter (January–March), summer (July–September) and annual SST data were extracted at a depth of 10 m from the World Ocean Atlas (WOA, vol. 2) (Kucera et al., 2004a), using the WOA 98 sample software (<http://www.palmod.uni-bremen.de/~csn/woasample.html>). The temperatures are calculated as the area-weighted averages of the four

WOA temperature points surrounding the sample location. An age quality level was assigned to each core top within the calibration data set following the criteria defined by the MARGO group (Kucera et al., 2004a). This is to investigate and eliminate the possible effects of residual glacial assemblages in surface sediments. The age quality levels ranged between 1 and 5 with level 1 indicative of core tops with the best chronological control, and level 5 the poorest. In instances where the quality of the core was borderline between two levels, the lower Chronozone quality level was selected. All of the data used in the calibration and LGM data sets are stored in the PANGAEA database (www.pangaea.de/Projects/MARGO).

Table 2
Details of unpublished core top samples added to the Mediterranean calibration data set

Core	Latitude	Longitude	Water depth (m)	Age quality	Faunal counts provided by
BS79-37	38.22	13.27	1458	4	Sbaffi
T87-11B	39.20	19.94	1322	2	Hayes
T87-14B	38.60	19.92	1999	2	Hayes
T87-43B	35.90	13.03	1514	2	Hayes
T87-45B	36.50	13.32	1716	2	Hayes
T87-65B	38.60	10.78	904	2	Hayes
T87-71B	38.90	10.59	2654	2	Hayes
T87-95B	39.00	9.28	499	2	Hayes
T87-108B	36.70	2.64	212	2	Hayes
T87-118B	37.00	2.55	2000	2	Hayes
T87-128B	35.50	-2.67	296	2	Hayes
T87-133B	35.80	-2.89	1100	2	Hayes
T83/20	31.60	29.61	790	2	Hayes
T83/25	32.20	29.29	2034	2	Hayes
T83/67	33.20	23.09	2075	2	Hayes
Ki06	37.46	11.55	885	5	Kallel
Ki201	41.35	5.13	2450	5	Kallel
Ki202	40.35	4.60	1870	5	Kallel
Ki203	37.08	5.26	2245	5	Kallel
Ki206	38.20	18.01	950	5	Kallel
Ki211	35.85	25.33	1835	5	Kallel
Ki307	36.43	-1.90	1420	5	Kallel
Ki320	36.01	-4.71	950	5	Kallel
1Ki02	37.98	4.10	1870	5	Kallel
1Ki04	37.05	7.37	2500	5	Kallel
1Ki08	35.75	18.45	3733	5	Kallel
1Ki11	33.76	32.71	946	5	Kallel
Ki5 & Ks5	37.73	8.60	1520	5	Kallel
K7 & Ks7	36.75	15.83	2500	5	Kallel
Ks 09	35.35	28.13	1330	5	Kallel
KS8233	36.20	-1.23	2500	5	Kallel
KC8240	35.55	-4.66	533	5	Kallel

2.2. Last glacial maximum data set

For the purpose of this paper, the LGM Chronozone is defined as the interval between 19,000 and 23,000 cal-yr BP (Mix et al., 2001) that includes the centre of the LGM event previously defined by CLIMAP (1976). Fig. 5 illustrates the 37 Mediterranean cores that were selected for this time slice. This data set includes 13 cores taken from Kallel et al. (1997b), 10 other previously published cores (Table 3) and new data from an additional 14 cores (Table 4). The cores used in Thiede's (1978) and Thunell's (1979) studies were not incorporated into our LGM data set since we were unable to trace them. Whilst the addition of these samples would have allowed a higher spatial resolution of the LGM reconstruction, by using only the 37 new cores we were able to ensure taxonomic consistency and a consistent minimum level of age control across this new LGM data set.

All samples falling within the LGM interval were selected in each core. A total of 273 samples were used ranging between 1 and 23 samples per core. The census counts of planktonic foraminifera from all the samples

included in the LGM data set are based on the > 150 µm size fraction using the same taxonomic concepts as applied in the calibration data set (Table 5). Counts were based, where possible, on suitable aliquots of approximately 300 specimens obtained using a random split. Each core was assigned an age quality level (1 indicating the highest quality level) according to the EPILOG criteria (Mix et al., 2001) expanded by the MARGO group (Kucera et al., 2005a). The LGM SST estimates for each core were obtained by calculating the average SST from all samples within the defined LGM interval. The standard deviation was calculated for those cores that contained two or more samples within the glacial interval, this included 35 cores within the LGM data set.

3. Methods

3.1. Artificial neural network

ANN, a branch of artificial intelligence, are computer systems that have the ability of unsupervised learning of

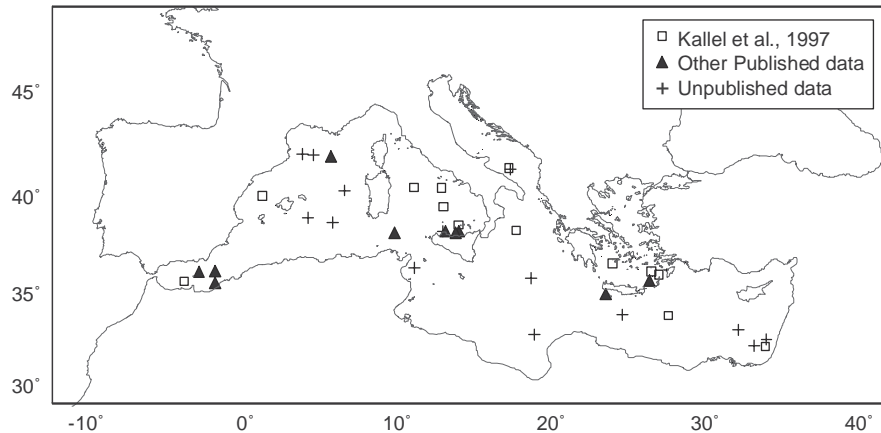


Fig. 5. Map illustrating the core localities in the LGM data set used in this study. Refer to Tables 3 and 4 for source details.

Table 3

Summary of cores used in the LGM data set taken from published sources in addition to those in Kallel (1997b)

Core	Latitude	Longitude	Water depth (m)	No. of samples	Age quality	Age model	Data source
T87/2/20G	34.97	23.75	707	3	2	a	Rohling and Gieskes (1989)
KS310	35.55	-1.57	1900	7	2	a	Rohling et al. (1995)
BC15	41.95	5.93	2500	3	2	a, b	Rohling et al. (1998)
LC07	38.14	10.07	488	3	3	b	Hayes et al. (1999)
LC21	35.66	26.58	1522	8	3	a, b	Hayes et al. (1999)
MD95-2043	36.14	-2.62	18.41	7	2	a, b	Cacho et al. (1999)
BS79-22	38.23	14.23	1449	21	3	b	Sbaffi et al. (2001)
BS79-33	38.16	14.02	1282	13	3	a, b	Sbaffi et al. (2001)
BS79-38	38.25	13.35	1489	24	3	b	Sbaffi et al. (2001)
ODP 977	36.19	-1.57	1984	5	3	a, b, c	Perez-Folgado et al. (2003)

a, AMS ^{14}C data; b, Oxygen isotope stratigraphy; c, biostratigraphy.

Table 4

Details of unpublished cores added to the LGM data set

Core	Latitude	Longitude	Water depth (m)	No. of samples in LGM interval	Age quality	Age model	Faunal counts provided by
ODP 969	33.84	24.88	2200	5	4	c	Hayes
ODP 973	35.78	18.94	3695	2	4	c	Hayes
ODP 975	38.89	4.50	2426	5	4	c	Hayes
LC01	40.26	6.89	2845	4	3	b	Hayes
LC04	38.65	6.11	2855	3	3	b	Hayes
BS79-37	38.22	13.27	1458	3	3	a	Sbaffi
MD84-627	32.14	33.45	1185	3	3	b	Kallel
MD84-632	32.47	34.23	14.5	19	3	b	Kallel
MD84-641	33.02	32.38	1375	6	1	a, b	Kallel
MD99-2346	42.04	4.15	2089	23	3	a, b	Kallel
MD90-917	41.30	17.61	1010	17	2	a, b	Kallel
MD99-2344	42.00	4.84	2326	4	3	a, b	Kallel
KET80-39	36.32	11.41	290	15	4	c	Kallel
KL96	32.77	19.19	1390	2	3	b	Hayes

a, AMS ^{14}C data; b, Oxygen isotope stratigraphy; c, biostratigraphy.

a relationship between two sets of variables (Wasserman, 1989). The general principles and architecture of backpropagation (BP) neural networks and its application to palaeoceanographic data are described in

Malmgren and Nordlund (1997) and Malmgren et al. (2001). A trained ANN can be best compared to a complicated, recurrent mathematical formula transforming input variables (species abundances) into

Table 5

List of planktonic foraminiferal species and taxonomic categories used in the calibration and LGM data sets

Species
<i>Orbulina universa</i>
<i>Globigerinoides conglobatus</i>
<i>Globigerinoides ruber</i> (pink and white)
<i>Globoturborotalita tenella</i>
<i>Globigerinoides sacculifer</i> (with and without sac)
<i>Sphaeroidinella dehiscentes</i>
<i>Globigerinella siphonifera</i> + <i>Globigerinella calida</i>
<i>Globigerina bulloides</i>
<i>Globigerina falconensis</i>
<i>Beella digitata</i>
<i>Globoturborotalita rubescens</i>
<i>Turborotalita quinqueloba</i>
<i>Neogloboquadrina pachyderma</i> sin.
<i>Neogloboquadrina dutertrei</i>
<i>Neogloboquadrina pachyderma</i> dex. + “P/D intergrades”
<i>Pulleniatina obliquiloculata</i>
<i>Globorotalia inflata</i>
<i>Globorotalia truncatulinoides</i>
<i>Globorotalia crassaformis</i>
<i>Globorotalia hirsuta</i>
<i>Globorotalia scitula</i>
<i>Globorotalia menardii</i> + <i>Globorotalia tumida</i>
<i>Globigerinita glutinata</i>

desired output variables (SST). A BP ANN consists of a series of processing units (neurons) arranged in layers where each neuron in a preceding layer is connected to all neurons of the following layer. The training of a BP ANN is accomplished by iterative adjustment of arrays of coefficients defining the output of each of the neurons. The adjustment of the coefficients is based on the change of total error rate between two individual iterations. ANNs can successfully learn complex, non-linear relationships and the technique is not as dependent on the size, coverage and balance of the calibration data set as the *k*-nearest-neighbour techniques (MAT, SIMMAX, RAM).

In this application, the calibration data set (274 samples) was randomly split into two representative sub-sets using the NeuroGenetic Optimizer (v2.6) program. The larger sub-set, comprising 80% of the samples (219 samples), was used for training, whilst the remaining 20% (55 samples) constituted the test sub-set. This splitting procedure was repeated 10 times to allow for a reliable estimate of prediction error and provide a means of assessing the dependency of the estimated values on small changes in the calibration data set. Training of the ANN was performed separately for annual, winter (January–March) and summer (July–September) SSTs. The best network in each of the 10 partitions has been retained and all SST reconstructions were calculated as averages of reconstructions produced by these 10 networks. In each partition, the prediction error of the

ANN technique, the root mean square error of prediction (RMSEP), was calculated as the square root of the sum of the squared differences between the observed and predicted values for all samples within the test set, divided by the number of samples (55 samples).

The NGO software uses a genetic algorithm to search for the parameters of the network that produce the lowest error of prediction (Malmgren et al., 2001). In this application, the maximum number of neurons per hidden layer was set at 16 in each of one or two hidden layers. Given the small number of samples in the calibration data set, training of larger networks would be severely underdetermined. For each partition, the algorithm searched through 30 generations with each population containing 100 neural network configurations, recording a total of 3000 network configurations per partition. The maximum number of learning epochs was set to 2500 for each configuration. If no improvement in the prediction error in the test set occurred after 30 consecutive epochs the network is instructed to stop. The parameters of the best networks for each temperature definition and partition are listed in Table 6.

3.2. Revised analogue method

Of the alternative methods available, we opted to use the RAM as a comparison for the ANN technique. IKTF is known to produce the largest errors amongst all the techniques (Malmgren et al., 2001), whilst both MAT and SIMMAX depend on large numbers of samples in the calibration data set. Additionally, SIMMAX includes a weighting procedure of the best analogues' SSTs according to the inverse geographical distances of the most similar samples (Pflaumann et al., 1996). This is problematic in the glacial Mediterranean where some of the best analogues are expected to derive from the North Atlantic. The RAM technique appears the most suitable alternative to ANN in the Mediterranean, as it may overcome the lack of samples in the calibration data set by the addition of virtual coretops and a restrictive selection of the number of best analogue samples.

RAM is a variant of MAT with several significant modifications (Waelbroeck et al., 1998). Like MAT, this method searches the calibration data set for the best analogues on the basis of a dissimilarity coefficient. In addition, for each sample RAM attempts to constrain the number of best analogues by searching for ‘jumps’ in the dissimilarity coefficient. The best analogues encountered prior to the first jump are retained; however, if no jumps are detected then a given number ($\beta = 10$ in this application) of analogues are kept. The second modification allows the calibration data set to be artificially expanded by mapping the original data onto a grid of environmental variables with a given mesh size (γ). The technique creates virtual faunal assemblages at each

Table 6
Configurations of the best artificial neural networks for each partition of the calibration dataset

Partition	RMSEP		1HL			2HL			Out	
	tst	trn	Lo	T	Li	Lo	T	Li		<i>N</i>
Summer										
1	1.1539	1.1027	7	5	5				1Li	17
2	1.1984	1.0302	6	6		2		2	1Li	16
3	1.0139	1.3570	1	1	1	4	2	3	1Li	12
4	1.2653	0.9637		6	5				1Li	11
5	0.9447	1.0918	1	2	8				1Li	11
6	1.2747	1.1227	4	5		3	2		1T	14
7	0.9818	1.1159	4	1	1				1Li	6
8	1.2495	1.0266	3	5	4	6	4	1	1Li	23
9	1.2325	1.1031	1	3					1Li	4
10	1.0784	1.0355		3	2				1Li	5
Average	1.1393	1.0949								12
Winter										
1	0.8486	0.6804	7	5					1Li	12
2	0.8030	0.6847	5	4	3				1Li	12
3	0.6524	0.6964	3	4	2				1Li	9
4	0.7444	0.617	11	2	2		2	14	1Li	31
5	0.6987	0.8582	6	3	2	7	5		1T	23
6	1.0584	0.805	2		2	1	1		1T	6
7	0.7415	0.6724	6	6	2		1	1	1Li	16
8	0.7686	0.6725	12	2		2	1	1	1Li	18
9	0.8868	0.6993	1	2	2				1Li	5
10	0.7286	0.8232	1	1					1Li	2
Average	0.7931	0.7209								13
Annual										
1	0.9947	0.844	9	2	4				1Li	15
2	0.9666	0.8374	6	6	2	1		1	1Lo	16
3	0.7891	0.9882	1	1	1	2	2	2	1Li	9
4	0.9598	0.8451	4	4					1Lo	8
5	0.742	0.8803		6	2				1Li	8
6	1.0708	0.7936	9	1	6		3	2	1Li	21
7	0.7677	0.804	4	4	7	3	2	2	1Li	22
8	0.9397	0.7816	2	3	2	1	1	2	1Li	11
9	0.9998	0.7931	11		5	2	3	1	1Li	22
10	0.8916	0.8434	2	2	3				1Li	7
Average	0.9122	0.8411								14

tst, test data (20% of data set); trn, training data (80% of data set); Lo, neurons with logarithmic transfer function; T, neurons with hyperbolic tangent transfer function; Li, neurons with linear transfer function; HL, hidden layer, Out, output layer; *N*, number of neurons in hidden layers.

node on the grid by interpolating abundances from the calibration data set within a given radius (*R*). A more detailed explanation of the RAM is described in Waelbroeck et al. (1998). For the purpose of this study we have opted to use the modified RAM02 software, which automatically selects the parameter related to the selection of the best analogues (α) (Kucera et al., 2005b). The interpolation procedure in RAM02 is constrained to two dimensions. In this study, we have used $\gamma = 0.25$ and $R = 0.3$, for summer vs. winter SST interpolation (following Waelbroeck et al., 1998) and an annual vs.

seasonality SST interpolation to produce independent estimates of annual SST. The RMSEP for RAM has been calculated by using the ‘leaving-one-out’ method; however, the RAM02 software leaves out the best analogue (i.e. itself) after the interpolation. Since the virtual core tops are based on the assemblages of the ‘left out’ sample the error estimates are inevitably underestimated.

4. Results and discussion

4.1. Calibration

The results of the calibration of both ANN and RAM are displayed in Figs. 6–8. For ANN, the average values of the 10 networks are shown for each SST reconstruction. The errors produced in this way (show as RMSE in Fig. 6) are slightly underestimated when compared to the average RMSEP values, which provide a better estimate of how the technique will perform on samples from outside of the calibration data set. Because of the way the RAM02 software performed the leaving-one-out validation (see above) the error rates reported for RAM (Fig. 6) are not fully comparable to ANN RMSEP values. Nevertheless, we observe a similar pattern where both techniques appear most successful in reconstructing winter SSTs and least successful in reconstructing summer SSTs. It is interesting to note that for all SST definitions, the error rate calculated by RAM for the entire data set is lower than that for the Mediterranean data set. The reverse pattern is observed for the ANN results, which record a lower error rate for the Mediterranean portion of the calibration data set (Fig. 6).

An examination of the residual values (i.e. observed minus predicted SST values) shows very little bias towards a systematic under or overestimating at any part of the SST range (Fig. 7A). As noted previously, the winter season temperatures are easier to reconstruct by both ANN and RAM, compared to summer or annual average values. Using the ANN technique, approximately 12% of the data set produced errors of $\pm 1^\circ\text{C}$, compared to 7% produced by RAM. The relatively weak correlation between residuals of each technique (Fig. 7B) suggests that ANN and RAM are predicting SSTs in a different manner. To assess the effect of age quality on the SST estimates, Fig. 8 shows the relationship between the residuals from each technique and the age quality of each core top. It is immediately obvious that age quality has no bias towards reducing the incidence of underestimated SST reconstructions. The only exception is observed in summer SST estimates by ANN, where quality level 3 cores show evidence of underestimation; the lack of core numbers within this category could account for this discrepancy. We

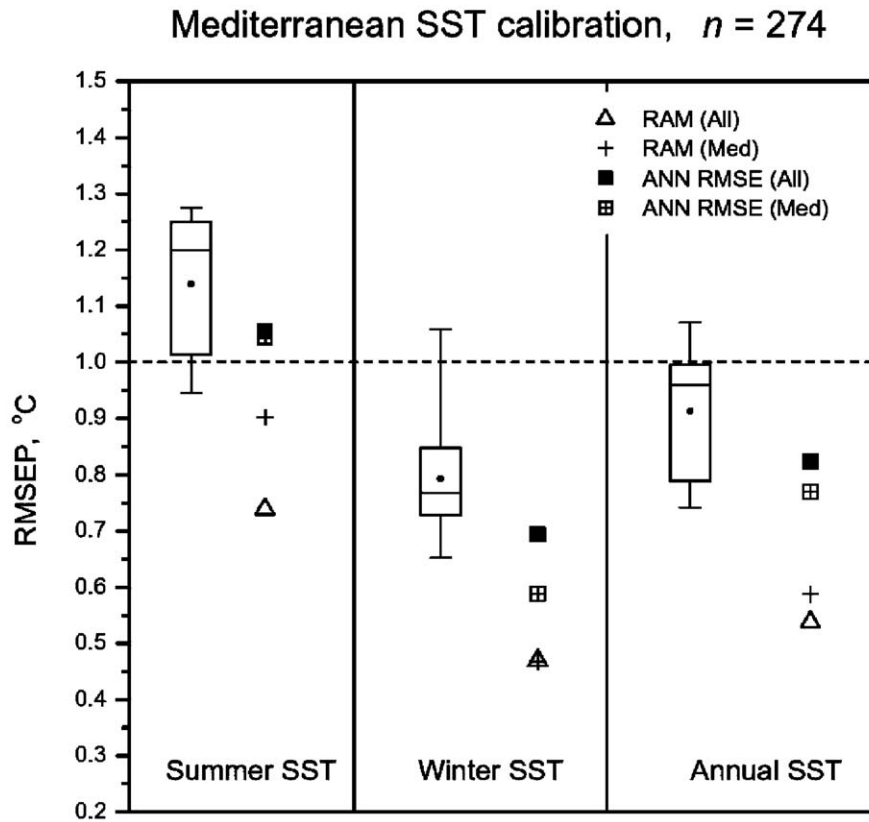


Fig. 6. Summary of the prediction errors produced by ANN and RAM. The box and whiskers plots show the minimum and maximum RMSEP values for ANN, along with the 0.25 percentile, median, mean (black dot) and 0.75 percentile. The ANN RMSE values were calculated from SST estimates based on average values of the ten best networks. The RAM error rate is based on leaving-one-out procedure applied after the two-dimensional interpolation; such error rate is therefore expected to be an underestimate of how the technique will perform outside of the calibration data set.

conclude that the calibration data set does not appear to be affected by samples with residual glacial assemblages.

4.2. Application to glacial samples

The SST estimates discussed in the following sections are determined by calculating the average SSTs from all samples contained within the LGM interval in each core. It should be noted that core KL96 (Table 4) does not contain SST estimates from RAM since no suitable analogues were found for the assemblages encountered in this core.

4.2.1. Glacial summer

The results of both RAM and ANN suggest that the SST gradient between the western and eastern basins was significantly greater during the LGM than today (Fig. 9). During the summer, with the exception of the Adriatic and Aegean Seas, the eastern Mediterranean was the warmer of the two basins with temperatures in the far east reaching $\sim 23^\circ\text{C}$. Surface waters at the Strait of Sicily and along the North African coast as far as the Balearic basin are estimated at $\sim 17^\circ\text{C}$. Cooler water conditions ($\sim 13^\circ\text{C}$) are observed extending southwards

from the Gulf of Lions (Fig. 9A). Westward into the Alboran Sea (western Mediterranean) SSTs were up to $\sim 14^\circ\text{C}$. The ANN estimates suggest a warm surface water anomaly ($\sim 16^\circ\text{C}$) off the east coast of Spain (Fig. 9A). The coldest part of the basin is observed in the Gulf of Lions where temperatures drop to $\sim 10^\circ\text{C}$, coinciding with the area of western Mediterranean deep water formation (WMDW) (MEDOC group, 1970). The southerly displacement of the isotherms in the eastern basin reflects an extension of cool conditions over the open basin from the Aegean Sea ($\sim 16^\circ\text{C}$) (Fig. 9A). The differences between the glacial and present day (WOA 98, vol. 2) summer SSTs expressed as a temperature anomaly are illustrated in Fig. 9B. From the distribution of summer anomalies it is evident that major temperature changes occurred in the western basin with temperatures dropping to 11°C below modern temperatures. Other significant changes are observed in the Adriatic and Aegean Seas recording temperature decreases of 6 and 7°C , respectively. Both of these areas contribute to the formation of eastern Mediterranean deep water (EMDW) today (Wüst, 1961; Miller, 1963; Roether et al., 1996), and given these coolings, likely did so in glacial times.

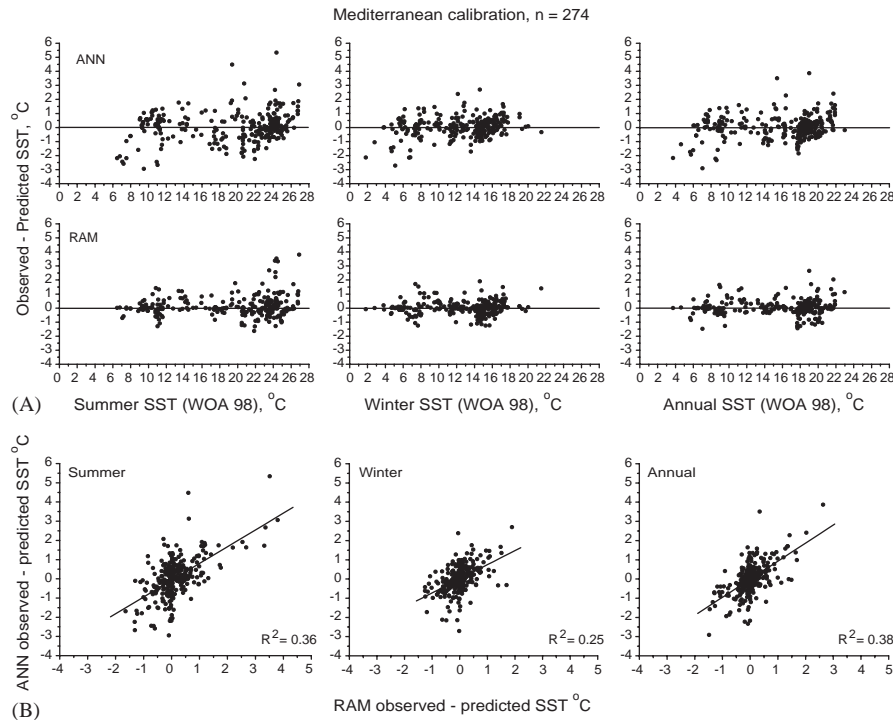


Fig. 7. (A) Relationships between observed and residual (i.e. observed–predicted) SSTs for summer, winter and annual temperatures in the calibration data set. (B) Relationship between SST residuals for ANN and RAM summer, winter and annual temperatures.

4.2.2. Glacial winter

Although the west–east temperature gradient was significantly stronger during the glacial winter than today, it was somewhat reduced compared to reconstructions for the glacial summer (Fig. 9A). The warmer eastern basin has a maximum temperature of $\sim 16^{\circ}\text{C}$, with cooler (13°C) surface water conditions observed in the Aegean Sea extending southwards into the Levantine basin. The Gulf of Lions remained the coldest part of the Mediterranean with temperatures dropping as low as $\sim 7^{\circ}\text{C}$. Winter temperature anomalies are less dramatic than those observed during the glacial summer (Fig. 9B). The major changes occurred in the western basin, particularly in the Alboran Sea and Gulf of Lions where SSTs are recorded at 6°C lower than modern winter temperatures. Once again the Aegean Sea was much cooler than today displaying a 5°C decrease during the glacial winter.

4.3. Comparison between ANN and RAM

In general, both ANN and RAM reconstructed similar isotherm patterns in the glacial Mediterranean. However, the ANN technique tends to reconstruct higher SSTs for both the summer and winter, by $1\text{--}2^{\circ}\text{C}$ (Fig. 9). The mean standard deviations of SST estimates between the 10 partitions (ANN) and the best analogues (RAM) are illustrated in Fig. 10. RAM produces higher standard deviations, particularly during

the glacial summer, with 91.6% of the cores recording a standard deviation above 1. This is only slightly reduced to 86.1% for the glacial winter. By comparison, the standard deviations above 1 for ANN are 62.2% and 40.5% for summer and winter, respectively. Generally, the ANN appears more consistent (i.e. lower standard deviations) in predicting warmer SSTs (Fig. 10—see samples indicated by a cross). Conversely, RAM produces its lowest standard deviations for cores located in the cooler Gulf of Lions (Fig. 10—see samples indicated by an open triangle). The high standard deviations produced by RAM reflect the variability of SSTs among the selected best analogues. Although RAM adds a number of virtual samples to expand the calibration data set, there still appears to be an insufficient number of samples with consistent SSTs between the selected best analogues.

By calculating the standard deviation of the mean SST predictions within the LGM interval, we can observe the stability of the LGM at each core location (Fig. 11A). It should be noted that there is no relationship between the standard deviation and the number of samples within the LGM interval. Both techniques suggest a similar degree of variability within the LGM, only during the glacial summer RAM produced higher standard deviations (paired *t*-test, $p < 0.05$) indicating greater SST variability, especially at two locations (Fig. 11A). Despite the limitations of this analysis given by the uneven numbers of samples

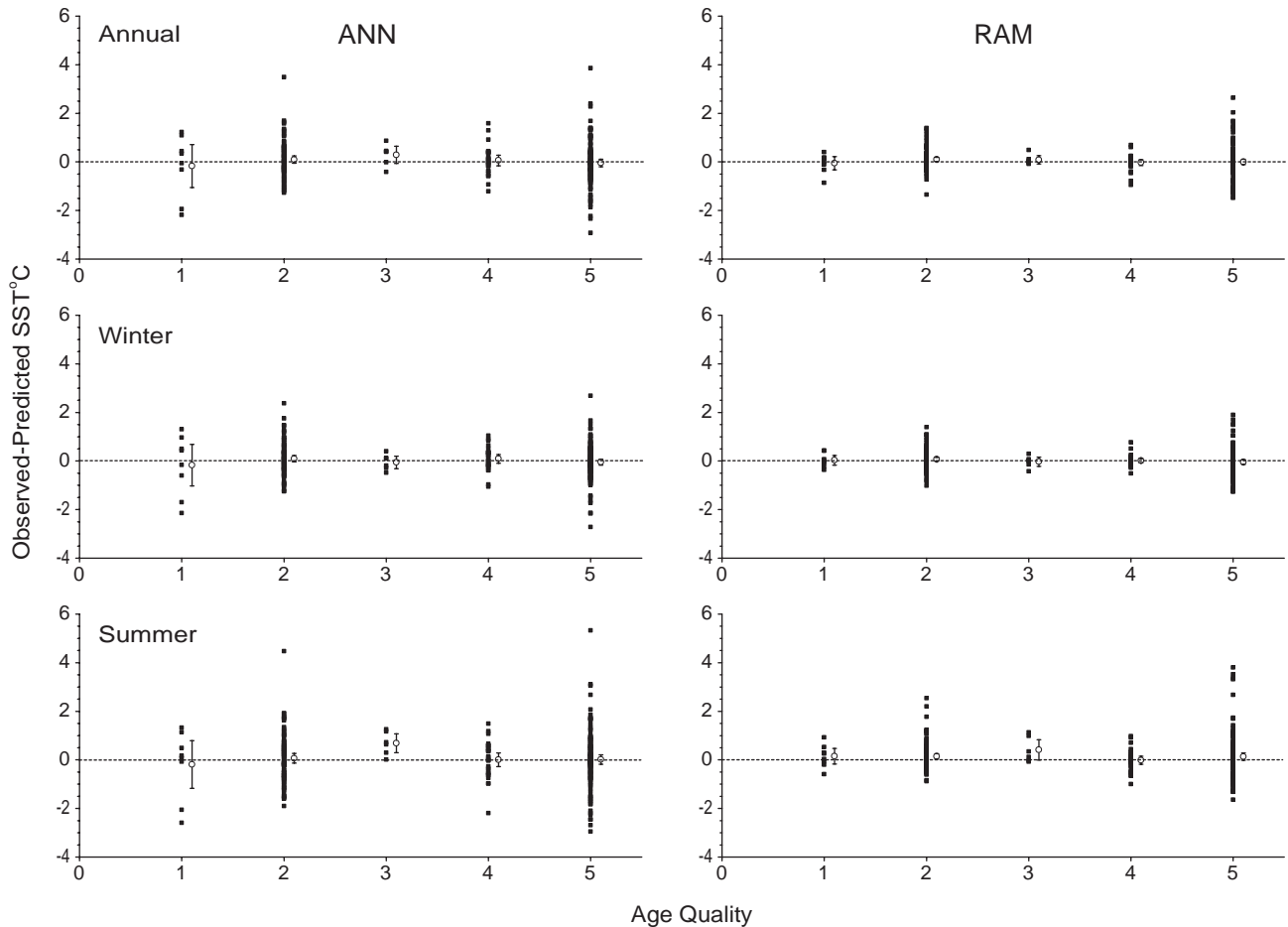


Fig. 8. Relationship between SST residuals and the age quality level of each core top sample in the calibration data set. Plots illustrate annual, summer and winter temperatures for both ANN and RAM methods. Open circles indicate the mean residual SST for each quality level. The error bars indicate the 95% confidence intervals. Quality levels range from 1 to 5 (1 being the best quality—see Kucera et al. (2004a) for full criteria).

per core in the LGM interval, the fact that some of the LGM variability clearly exceeds the expected prediction errors (Fig. 6) suggests a significant LGM instability in the Mediterranean, centred on areas with SST values in the middle of the glacial Mediterranean range.

Although the lack of consistency among the selected best analogues seems to be affecting RAM SST reconstructions, both the ANN and RAM techniques have produced similar SST patterns during the LGM (Fig. 11B). With this in mind, further discussions will relate only to SST estimates derived using ANN. The effect of the quality of dating of glacial samples on the coherence of SST reconstructions is shown in Fig. 12. In the southeastern Mediterranean, a core with a well-constrained chronological timeframe (level 1) produced a similar SST prediction to three other cores from the same region with age quality level 3. This highlights a general observation that samples from less well-dated cores do not deviate from regional patterns suggested by samples from cores with the best available chronology.

4.4. Comparison with previous LGM SST reconstructions

Although there are obvious similarities, our glacial SST reconstructions display some significant differences compared to previous studies based on the IKTF technique in the Mediterranean Sea. During the glacial summer, using the ANN technique, SST reconstructions range from 14 °C in the Alboran Sea to 23 °C in the south east of the basin, giving an SST gradient of 9 °C. This differs from initial reconstructions proposed by CLIMAP (1976) who estimated the SST gradient at 12 °C, while Thiede (1978) suggested that it was between 6 and 12 °C. The ANN SST estimates in the eastern basin tend to be 2–3 °C lower than those suggested by both CLIMAP (1976) and Thiede (1978). A similar deficit is noted in comparison with glacial reconstructions conducted by Thunell (1979). Although the ANN estimates in the western basin are in general agreement with CLIMAP (1976), there are some significant disagreements with Thiede's (1978) data. In the Gulf

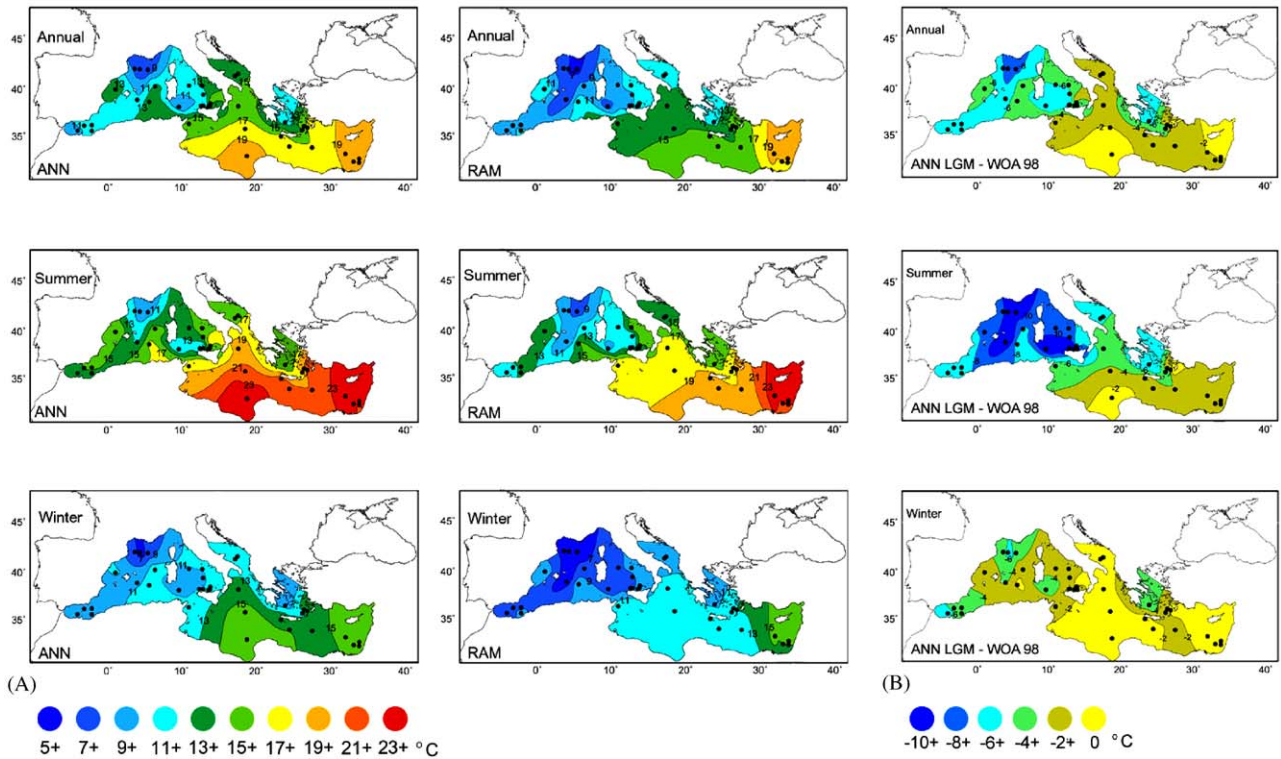


Fig. 9. (A) Glacial annual, summer and winter SST reconstructions based on ANN and RAM. (B) Temperature anomalies for annual, summer and winter SSTs during the last glacial maximum. Values are derived by subtracting modern day SSTs (World Ocean Atlas 98 v2) from glacial values, based on ANN reconstructions. The contour lines were created using the nearest neighbour option in the MapInfo Professional software (version 6.5). Black dots indicate location of cores used for reconstructions. Since we only aimed to produce a schematic representation of LGM SSTs, it should be noted that the base map does not take into account the lowered sea level during the LGM.

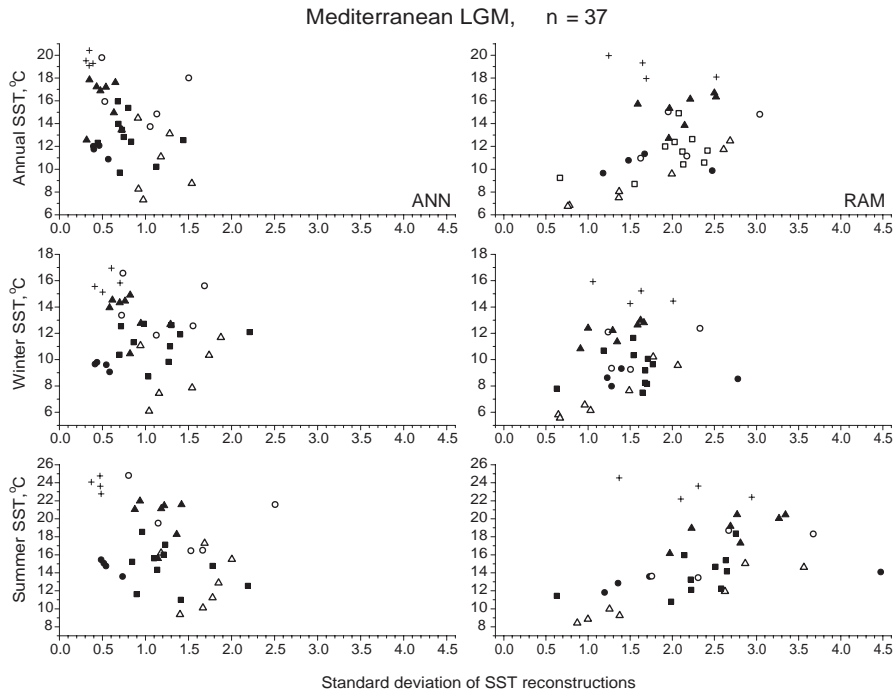


Fig. 10. The mean standard deviations of SST estimates between the 10 partitions (ANN) and the best analogues (RAM) plotted against glacial annual, summer and winter SSTs. Closed circle = Alboran Sea; open triangle = Gulf of Lions/Balearic basin; closed square = Tyrrhenian Sea/Strait of Sicily; open circle = Central Mediterranean; closed triangle = Southern Aegean Sea/Levantine basin; cross = Far eastern Mediterranean.

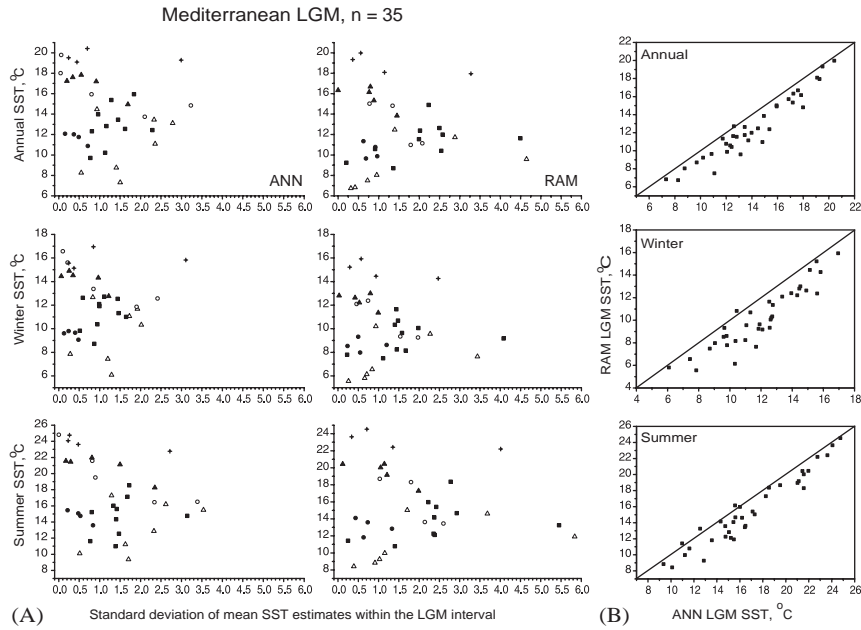


Fig. 11. (A) Relationship between glacial annual, summer and winter SSTs and the standard deviation of the SST predictions within the LGM interval for both ANN and RAM. Cores containing only one sample within the LGM are omitted. For key to symbols refer to Fig. 10 caption. (B) Relationship between LGM SSTs for ANN and RAM summer, winter and annual temperatures.

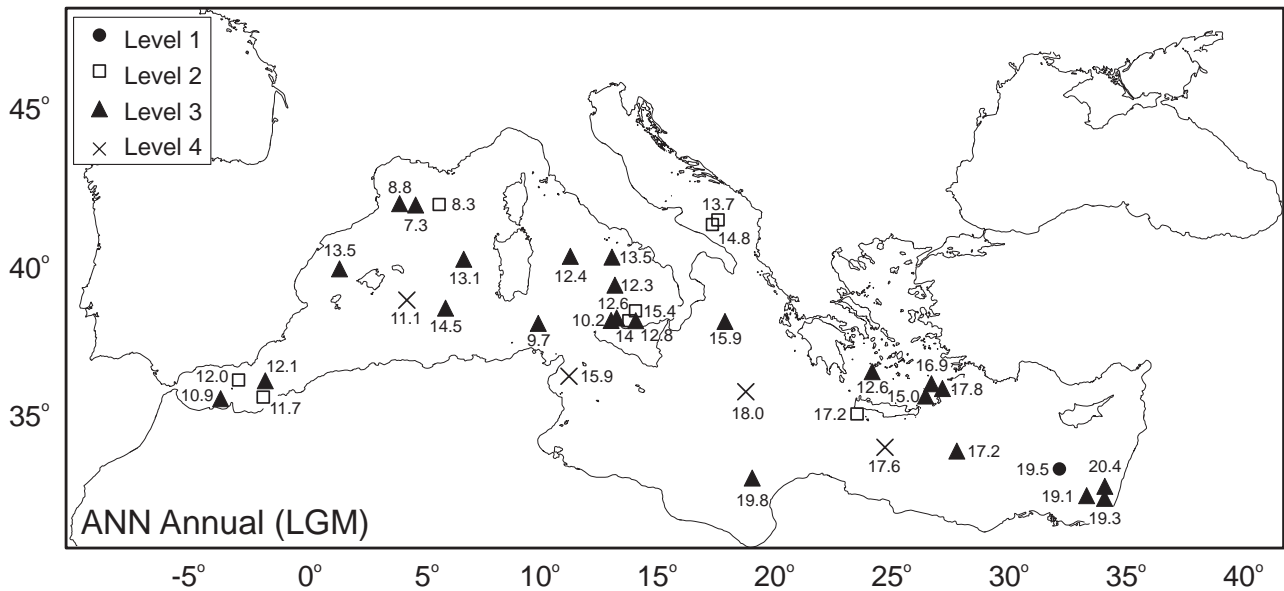


Fig. 12. The coherency of SST reconstructions in cores with different chronological control. Symbols indicate the age quality level (1–4) (Kucera et al., 2004a) of each core within the LGM data set. Values indicate annual SSTs based on ANN estimates.

of Lions, Thiede (1978) estimates an SST between 13–15 °C in contrast to ANN estimates of ~10 °C. The most notable differences occur in the Alboran Sea. According to Thiede (1979) a north–south gradient of 6 °C (13–19 °C) existed in the glacial summer in the Alboran Sea, equalling that estimated for the entire basin (Fig. 2B). In contrast, the ANN summer reconstructions suggest an average SST of 14 °C in the

entire Alboran Sea. This is in agreement with Perez-Folgado et al. (2003) who estimated a glacial summer SST of ~14 °C based on two cores in the Alboran Sea, using the modern analogue technique. Similarly, estimates produced by alkenone studies suggest SSTs between 11.5 and 13 °C during the LGM in the Alboran Sea (Cacho et al., 2000; Perez-Folgado et al., 2003). These compare well to our annual estimates of ~12 °C.

All reconstructions observe a SST decrease in the Aegean Sea. Both CLIMAP (1976) and Thunell (1979) suggest a reduction of approximately 1 °C (22 °C) relative to the present day, whereas Thiede (1978) and our ANN estimates indicate a more significant decrease of 7 °C (Fig. 9B).

The west–east SST gradient in the Mediterranean was significantly reduced during the glacial winter, with ANN estimating a value of just 6 °C compared to between 10 and 12 °C suggested by Thiede (1978). The ANN estimates in the eastern basin tend to be 2–3 °C higher than temperatures proposed by Thunell (1979), yet some 2–4 °C lower than Thiede's (1978) reconstructions. The Aegean Sea provides the exception with ANN SST estimates of 11 °C, comparable to that of Thiede (1978) but approximately 3 °C higher than those suggested by Thunell (1979). Smaller discrepancies occur within the western basin with both the ANN and Thiede's (1979) reconstructions differing within 1–2 °C, which is close to the estimated error of prediction for the ANN (Fig. 6).

All previous glacial SST reconstructions, including data from this study are summarised in Fig. 13. During the glacial summer it is interesting to note that CLIMAP (1976) and Thiede (1978) estimate that SSTs in the eastern basin were the same or within 1 °C of modern day values. In the western basin, with the exception of Thiede (1978), both CLIMAP (1976) and this study indicate a cooling of approximately 6 °C compared to

the present day. Conversely, during the glacial winter there is more variability within the SST reconstructions across the entire basin (Fig. 13). From all previous reconstructions, our results generally compare well with estimates proposed by CLIMAP (1976). However, a more precise comparison is difficult since the geographical resolution of cores used by CLIMAP (1976) is poor, therefore providing only a broad overview of the glacial Mediterranean. Compared to Thiede (1978), our ANN reconstructions only agree with winter reconstructions in the western basin and in the Aegean Sea during both seasons. This is expected since the calibration data set on which Thiede (1978) based his reconstructions only contained North Atlantic samples. This poses a problem for SST reconstructions in the eastern Mediterranean since the calibration data set contains no modern analogues for this region. As North Atlantic faunal assemblages are more similar to those in the cooler western basin, it is not surprising that Thiede's (1978) SST reconstructions from this region are more comparable with our results. Finally when compared with Thunell's (1979) reconstructions in the eastern Mediterranean, the ANN estimates are slightly lower in the summer and higher in the winter. These differences can probably be attributed to the core coverage of the reconstructions by Thunell (1979), which did not include any cores from the far eastern Mediterranean (see Figs. 2 and 5).

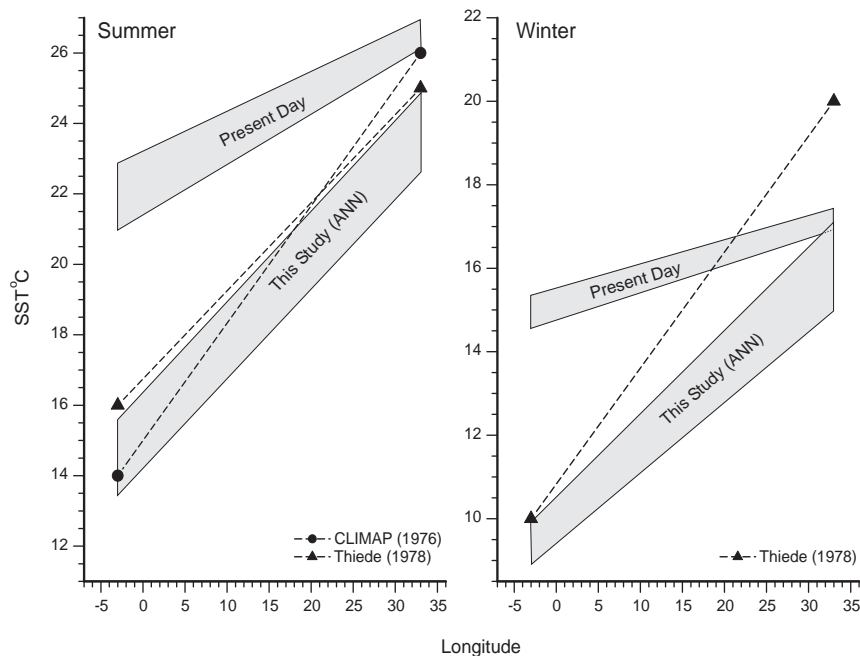


Fig. 13. A summary of Mediterranean east–west LGM temperature gradients reconstructed in this study and previous studies compared to present day gradients. Gradients for both summer and winter seasons are based on SSTs in the Alboran Sea and the south east Mediterranean. The grey shaded areas illustrate the range of SST gradients for both this study and the present day, whereas the gradients reconstructed for CLIMAP (1976) and Thiede (1978) are based on the average SST values.

4.5. Implications for models

Glacial SST reconstructions provide a means of testing ocean general circulation models. Previous attempts to model the circulation of the Mediterranean during the LGM have been conducted by Bigg (1994) and Myers et al. (1998). Bigg (1994) based his model on composite LGM SST reconstructions taken from Thiede (1978) and Thunell (1979). By comparison, Myers et al. (1998) opted to use the most extreme LGM SST estimates, using SST anomalies of -8°C in the north western basin (Rohling et al., 1998), -7°C in the central basin (Paterne et al., 1998) and -1°C in the southern extremity of the eastern basin (Paterne et al., 1998). Our LGM SST reconstructions, as explained previously, differ from Thiede (1978) and Thunell (1979) but are more comparable to those by Rohling et al. (1998) in the northwestern basin and Paterne et al. (1998) in the central Mediterranean. However, in the southeastern basin our results observe LGM SSTs $2\text{--}3^{\circ}\text{C}$ colder compared to 1°C colder as estimated by Paterne et al. (1998).

The LGM simulation produced by Bigg (1994) suggests an annual cooling in the eastern basin of 2°C . This compares well with our estimates; however, the simulation fails to observe the dramatic cooling that occurs in the Aegean Sea. On the other hand, the western basin is significantly underestimated observing an annual cooling of only 4°C compared to 7°C based on the ANN. By comparison, Myers et al. (1998) concluded that simulations for the LGM only produced significant SST changes in the western Mediterranean. It is difficult to compare our SST estimates with those of Myers et al. (1998) since the LGM simulation is specific to January, whereas the ANN calculates average winter SSTs. However, a strong similarity exists between both SST estimates in the western basin, although in the far south east of the basin the simulation suggests a maximum SST of 13°C compared to 16°C based on ANN. The absence of a consistent and reliable LGM data set is evident when using SST reconstructions within modelling applications. Previous attempts at modelling the glacial Mediterranean are either based on outdated SST reconstructions or a combination of individual studies.

5. Conclusions

To produce more precise and reliable reconstruction of glacial SSTs in the Mediterranean we compiled a new, more comprehensive calibration data set consisting of 129 core tops from the North Atlantic (Fig. 3) and 145 from the Mediterranean Sea (Fig. 4). Annual, summer and winter SSTs have been estimated using both ANN

and RAM methodologies, with average error rates ranging between 1.1 and 0.5°C (Fig. 6).

Glacial reconstructions are based on the largest ever LGM data set (Fig. 5), consisting of 273 samples in 37 cores, including new data for 12 cores. During the glacial summer, our reconstructions indicate a basin-wide east–west gradient of $\sim 9^{\circ}\text{C}$, whilst a gradient of 6°C is suggested for the glacial winter. Unlike previous studies, our ANN SST estimates suggest a significantly cooler (3°C) eastern basin during the glacial summer compared to the present day. In the western basin, ANN results are comparable to CLIMAP (1976) but disagree significantly with Thiede (1978). A significant decrease in SSTs has been confirmed in the Aegean Sea during the LGM. ANN SST estimates are much lower in the eastern basin compared to Thiede (1978) yet significantly higher (2°C) than values suggested by Thunell (1979). SST anomalies in the western basin are much lower during the winter and compare well to estimates proposed by Thiede (1978). SST estimates following the RAM technique produce comparable LGM reconstructions to ANN estimates in terms of magnitude and gradients; however, estimates tend to be $\sim 1^{\circ}\text{C}$ lower than those using the ANN technique. This discrepancy is comparable to our estimate of prediction errors of both techniques and we attribute it to an insufficient number of core tops within the calibration data set leading to the lack of consistency in SST values among the best-selected analogues. The reliability of our results is strengthened by the concordance of both techniques in extracting similar glacial SST patterns within the Mediterranean Sea. However, transfer function techniques such as RAM and MAT would benefit from larger calibration data sets.

Previous model simulations of the glacial Mediterranean relied on SST reconstructions that have become outdated. To overcome this problem, we constructed a larger calibration data set with a better constrained geographical range and a defined age quality control. Additionally, we used two modern transfer function techniques that produce lower RMSEP estimates and better generalisations than traditional techniques. Finally, the introduction of the largest-ever Mediterranean LGM data set combined with an enhanced age control on the definition of the LGM allowed us to provide modellers with a new set of targets on which to test simulations.

Acknowledgements

We would like to thank Simon Troelstra, Babette Hoogakker and Ralf Schiebel for providing samples and Mara Weinelt for running RAM on all the data. This project was funded by the Leverhulme Trust, the Nuffield Foundation and NERC. Thanks are due to

three anonymous referees for their constructive and helpful criticism of the first version of this paper.

References

- Bigg, G.R., 1994. An ocean general circulation model view of the glacial Mediterranean thermohaline circulation. *Paleoceanography* 9, 705–722.
- Buccheri, G., Capretto, G., Donato, V., Esposito, P., Ferruzza, G., Pescatore, T., Ermolli, E., Senatore, M., Sprovieri, M., Bertoldo, M., Carella, D., Madonia, G., 2002. A high resolution record of the last deglaciation in the southern Tyrrhenian Sea: environmental and climatic evolution. *Marine Geology* 186, 447–470.
- Cacho, I., Grimalt, J.O., Pelejero, C., Canals, M., Sierro, F.J., Flores, J.A., Shackleton, N., 1999. Heinrich event imprints in Alboran Sea paleotemperatures. *Paleoceanography* 14, 698–705.
- Cacho, I., Grimalt, J.O., Sierro, F.J., Shackleton, N., Canals, M., 2000. Evidence for enhanced Mediterranean thermohaline circulation during rapid climatic coolings. *Earth and Planetary Science Letters* 183, 417–429.
- Cita, M.B., Vergnaud-Grazzini, C., Robert, C., Chamley, H., Ciaranfi, N., d'Onofrio, S., 1977. Palaeoclimatic record of a long deep sea core from the eastern Mediterranean. *Quaternary Research* 8, 205–235.
- CLIMAP, 1976. The surface of the Ice-Age Earth. *Science* 191, 1131–1137.
- Gonzalez-Donoso, J., Serrano, F., Linares, D., 2000. Sea surface temperature during the Quaternary at ODP sites 976 and 975 (western Mediterranean). *Palaeogeography, Palaeoclimatology, Palaeoecology* 162, 17–44.
- Hayes, A., Rohling, E.J., De Rijk, S., Kroon, D., Zachariasse, W.J., 1999. Mediterranean planktonic foraminiferal faunas during the last glacial cycle. *Marine Geology* 153, 239–252.
- Herman, Y., 1972. Quaternary eastern Mediterranean sediments: micropalaeontological climatic record. In: Stanley, D.J. (Ed.), *The Mediterranean Sea*. Dowden, Hutchinson & Ross, Stroudsburg, PA, pp. 129–147.
- Hutson, W.H., 1980. The Agulhas current during the Late Pleistocene: analysis of modern faunal analogs. *Science* 207, 64–66.
- Imbrie, J., Kipp, J.Z., 1971. A new micropalaeontological method for quantitative paleoclimatology: application to a Late Pleistocene Caribbean core. In: Turekian, K.K. (Ed.), *The Late Cenozoic Glacial Ages*. Yale University Press, New Haven, pp. 71–181.
- Jorissen, F.J., Asioli, A., Borsetti, A.M., Capotondi, L., De Visscher, J.P., Hilgen, F.J., Rohling, E.J., Van der Borg, K., Vergnaud-Grazzini, C., Zachariasse, W.J., 1993. Late Quaternary central Mediterranean biochronology. *Marine Micropaleontology* 21, 169–189.
- Kallel, N., Paterne, M., Duplessy, J., Vergnaud-Grazzini, C., Pujol, C., Labeyrie, L., Arnold, M., Fontugne, M., Pierre, C., 1997b. Enhanced rainfall in the Mediterranean region during the last sapropel event. *Oceanologica Acta* 20, 697–712.
- Kucera, M., Darling, K.F., 2002. Cryptic species of planktonic foraminifera: their effect on palaeoceanographic reconstructions. *Philosophical Transactions of the Royal Society of London* 360, 695–718.
- Kucera, M., Rosell-Melé, A., Schneider, R., Waelbroeck, C., Weinelt, M., 2005a. Multiproxy approach for the reconstruction of the glacial ocean surface (MARGO). *Quaternary Science Reviews*, this issue (doi:10.1016/j.quascirev.2004.07.017).
- Kucera, M., Weinelt, M., Mara, K., Kiefer, T., Pflaumann, U., Hayes, A., Weinelt, M., Martin, Chen, M.-T., Mix, A.C., Barrows, T.T., Cortijo, E., Duprat, J., Juggins, S., Waelbroeck, C., 2005b. Reconstruction of the glacial Atlantic and Pacific sea-surface temperatures from assemblages of planktonic foraminifera: multi-technique approach based on geographically constrained calibration datasets. *Quaternary Science Reviews*, this issue (doi:10.1016/j.quascirev.2004.07.014).
- Lacombe, H., Gascard, J.C., Gonella, J., Bethoux, J.P., 1981. Response of the Mediterranean to the water and energy fluxes across its surface, on seasonal and inter-annual scales. *Oceanologica Acta* 4, 247–255.
- Lacombe, H., Richez, C., 1982. The regimes of the Straits of Gibraltar. In: Nihoul, J.C.J. (Ed.), *Hydrodynamics of Semi-enclosed Seas*. Elsevier, Amsterdam, pp. 13–74.
- Malmgren, B.A., Nordlund, U., 1997. Application of artificial neural networks to paleoceanographic data. *Palaeogeography, Palaeoclimatology, Palaeoecology* 136, 359–373.
- Malmgren, B.A., Kucera, M., Nyberg, J., Waelbroeck, C., 2001. Comparison of statistical and artificial neural networks for estimating past sea surface temperatures from planktonic foraminifer census data. *Paleoceanography* 16 (5), 520–530.
- MEDOC group, 1970. Observation of deep water formation in the Mediterranean Sea. *Nature* 227, 1037–1040.
- Miller, A.R., 1963. Physical oceanography of the Mediterranean Sea: a discourse. *Rapp. PV CIESM* 17, 857–871.
- Mix, A.C., Bard, E., Schneider, R., 2001. Environmental processes of the ice age: land, oceans, glaciers (EPILOG). *Quaternary Science Reviews* 20, 627–657.
- Molina-Cruz, A., Thiede, J., 1978. The glacial eastern boundary current along the Atlantic Eurafican continental margin. *Deep-Sea Research* 25, 337–356.
- Murray, J., 1897. On the distribution of the pelagic foraminifera at the surface and on the floor of the ocean. *Natural Science (Ecology)* 11, 17–27.
- Myers, P.G., Haines, K., Rohling, E.J., 1998. Modeling the paleocirculation of the Mediterranean: The last glacial maximum and the Holocene with emphasis on the formation of sapropel S₁. *Paleoceanography* 13 (6), 586–606.
- Myers, P.G., Rohling, E.J., 2000. *Quaternary Research* 53, 98–104.
- Olausson, E., 1960. Descriptions of sediment from the Mediterranean and Red Sea. *Reports of the Swedish Deep Sea Expedition, 1947–48* 8 (5), 287–334.
- Olausson, E., 1961. Studies of deep sea cores. *Reports of the Swedish Deep Sea Expedition, 1947–48* 8 (4), 353–391.
- Parker, F.L., 1958. Eastern Mediterranean foraminifera. *Reports of the Swedish Deep Sea Expedition, 1947–48* 8, 217–283.
- Paterne, M., Guichard, F., Labeyrie, J., Gillot, P.Y., Duplessy, J.C., 1986. Tyrrhenian Sea tephrochronology of the oxygen isotope record for the past 60,000 years. *Marine Geology* 72, 259–285.
- Paterne, M., Duplessy, J.C., Kallel, N., Labeyrie, J., 1998. CLIVAMP last glacial maximum sea salinities and temperatures, Technical Reports CLIVAMP-MAS3-CT95-0043, European Union Marine Science and Technology Program, Gif-sur-Yvette, France.
- Perez-Folgado, M., Sierro, F.J., Flores, J.A., Cacho, I., Grimalt, J.O., Zahn, R., Shackleton, N., 2003. Western Mediterranean planktonic foraminifera events and millennial climatic variability during the last 70 kyr. *Marine Micropaleontology* 48, 49–70.
- Pistek, P., De Strobel, F., Montanari, C., 1985. Deep Sea circulation in the Alboran Sea. *Journal of Geophysical Research* 90, 4969–4976.
- Pflaumann, U., Duprat, J., Pujol, C., Labeyrie, L., 1996. SIMMAX: a modern analog technique to deduce Atlantic sea surface temperatures from planktonic foraminifera in deep-sea sediments. *Paleoceanography* 11 (1), 15–35.
- Pflaumann, U., Sarnthein, M., Hapman, M., d'Abreu, L., Funnell, B., Huels, M., Kiefer, T., Maslin, M., Schulz, H., Swallow, J., van Kreveld, S., Vautravers, M., Vogelsang, E., Weinelt, M., 2003. Glacial North Atlantic: Sea-surface conditions reconstructed by GLAMAP 2000. *Paleoceanography* 18 (3), 1065.
- Pujol, C., Vergnaud-Grazzini, C., 1989. Paleoceanography of the last deglaciation in the Alboran Sea (Western Mediterranean). *Stable*

- isotopes and planktonic foraminiferal records. *Marine Micropaleontology* 15, 253–267.
- Roether, W., Manca, B.B., Klein, B., Bregant, D., Georgopoulos, D., Beitzel, V., Kovacevic, V., Luchetta, A., 1996. Recent changes in eastern Mediterranean deep waters. *Science* 271, 333–336.
- Rohling, E.J., Gieskes, W.W.C., 1989. Late Quaternary changes in Mediterranean intermediate water density and formation rate. *Paleoceanography* 4, 531–545.
- Rohling, E.J., Jorissen, F.J., Vergnaud-Grazzini, C., Zachariasse, W.J., 1993a. Northern Levantine and Adriatic Quaternary planktic foraminifera; reconstruction of paleoenvironmental gradients. *Marine Micropaleontology* 21, 191–218.
- Rohling, E.J., den Dulk, M., Pujol, C., Vergnaud-Grazzini, C., 1995. Abrupt hydrographic changes in the Alboran Sea (Western Mediterranean) around 8000 yrs BP. *Deep-Sea Research* 42, 1609–1619.
- Rohling, E.J., Hayes, A., Kroon, D., De Rijk, S., Zachariasse, W.J., 1998. Abrupt cold spells in the Late Quaternary NW Mediterranean. *Paleoceanography* 13 (4), 316–322.
- Sarthein, M., Gersonde, R., Niebler, S., Pflaumann, U., Spielhagen, R., Thiede, J., Wefer, G., Weinelt, M., 2003. Overview of Glacial Atlantic Ocean Mapping (GLAMAP 2000). *Paleoceanography* 18 (2), 1030.
- Sbaffi, L., Wezel, F.C., Kallel, N., Paterne, M., Cacho, I., Ziveri, P., Shackleton, N., 2001. Response of the pelagic environment to Palaeoclimatic changes in the central Mediterranean Sea during the Late Quaternary. *Marine Geology* 178, 39–62.
- Schott, W., 1935. Die Foraminiferen aus dem aequatorialen Teil des Atlantischen Ozeans. *Deutsch. Atl. Exped. Meteor. 1925–1927* 3, 34–134.
- Thiede, J., 1978. A glacial Mediterranean. *Nature* 276, 680–683.
- Thunell, R.C., 1978. Distribution of recent planktonic foraminifera in surface sediments of the Mediterranean Sea. *Marine Micropaleontology* 3, 147–173.
- Thunell, R.C., 1979. Eastern Mediterranean Sea during the last glacial maximum; an 18,000-years B.P. reconstruction. *Quaternary Research* 11, 353–372.
- Todd, R., 1958. Foraminifera from western deep-sea cores. Report of the Swedish Deep Sea Expedition, 1946–47 8, 167–215.
- Ufkes, E., Jansen, J.H.F., Brummer, G.J., 1998. Living planktonic foraminifera in the eastern South Atlantic during spring: indicators of water masses, upwelling and Congo (Zaire) River plume. *Marine Micropaleontology* 33, 27–53.
- Vergnaud-Grazzini, C., Ryan, W.B.F., Cita, M.B., 1977. Stable isotope fractionation, climatic change and episodic stagnation in the eastern Mediterranean during the Late Quaternary. *Marine Micropaleontology* 2, 353–370.
- Waelbroeck, C., Labeyrie, L., Duplessy, J., Guiot, J., Labracherie, M., Leclaire, H., Duprat, J., 1998. Improving past sea surface temperature estimates based on planktonic fossil faunas. *Paleoceanography* 13 (3), 272–283.
- Wasserman, P.D., 1989. *Neural Computing—Theory and Practice*. Van Nostrand Reinhold, New York 230pp.
- Wüst, G., 1961. On the vertical circulation of the Mediterranean Sea. *Journal of Geophysical Research* 66, 3261–3271.